

A Covalent Organic Framework Bearing Single Ni Sites as a Synergistic Photocatalyst for Selective Photoreduction of CO₂ to CO

Wanfu Zhong, Rongjian Sa, Liuyi Li, Yajun He, Lingyun Li,
Jinhong Bi, Zanyong Zhuang, Yan Yu, and Zhigang Zou

J. Am. Chem. Soc., **Just Accepted Manuscript** • DOI: 10.1021/jacs.9b02997 • Publication Date (Web): 18 Apr 2019

Downloaded from <http://pubs.acs.org> on April 18, 2019

Just Accepted

“Just Accepted” manuscripts have been peer-reviewed and accepted for publication. They are posted online prior to technical editing, formatting for publication and author proofing. The American Chemical Society provides “Just Accepted” as a service to the research community to expedite the dissemination of scientific material as soon as possible after acceptance. “Just Accepted” manuscripts appear in full in PDF format accompanied by an HTML abstract. “Just Accepted” manuscripts have been fully peer reviewed, but should not be considered the official version of record. They are citable by the Digital Object Identifier (DOI®). “Just Accepted” is an optional service offered to authors. Therefore, the “Just Accepted” Web site may not include all articles that will be published in the journal. After a manuscript is technically edited and formatted, it will be removed from the “Just Accepted” Web site and published as an ASAP article. Note that technical editing may introduce minor changes to the manuscript text and/or graphics which could affect content, and all legal disclaimers and ethical guidelines that apply to the journal pertain. ACS cannot be held responsible for errors or consequences arising from the use of information contained in these “Just Accepted” manuscripts.

A Covalent Organic Framework Bearing Single Ni Sites as a Synergistic Photocatalyst for Selective Photoreduction of CO₂ to CO

Wanfu Zhong^{†, #}, Rongjian Sa^{‡, #}, Liuyi Li^{†, *}, Yajun He[†], Lingyun Li[†], Jinhong Bi[†], Zanyong Zhuang[†], Yan Yu^{†, *}, Zhigang Zou^{†, §, *}

[†] Key Laboratory of Eco-materials Advanced Technology, College of Materials Science and Engineering, Fuzhou University, Fuzhou 350108, China.

[‡] Institute of Oceanography, Ocean College, Minjiang University, Fuzhou, Fujian 350108, China.

[§] Eco-materials and Renewable Energy Research Center, College of Engineering and Applied Sciences, Nanjing University, Nanjing 210093, China.

Supporting Information Placeholder

ABSTRACT: Photocatalytic reduction of CO₂ into energy-rich carbon compounds has attracted increasing attention. However, it is still challenge to selectively and effectively convert CO₂ to a desirable reaction product. Herein, we report a design of a synergistic photocatalyst for selective reduction of CO₂ to CO by using a covalent organic framework bearing single Ni sites (Ni-TpBpy), in which electrons transfer from photosensitizer to Ni sites for CO production by the activated CO₂ reduction under visible-light irradiation. Ni-TpBpy exhibits an excellent activity, giving a 4057 μmol g⁻¹ of CO in a 5 h reaction with a 96% selectivity over H₂ evolution. More importantly, when the CO₂ partial pressure was reduced to 0.1 atm, 76% selectivity for CO production is still obtained. Theoretical calculations and experimental results suggest that the promising catalytic activity and selectivity are ascribed to synergistic effects of single Ni catalytic sites and TpBpy, in which the TpBpy not only serves as a host for CO₂ molecules and Ni catalytic sites but also facilitates the activation of CO₂ and inhibits the competitive H₂ evolution.

■ INTRODUCTION

Visible-light-driven CO₂ reduction to useful chemical feedstocks is a promising strategy to utilize CO₂ and simultaneously store solar energy.^{1, 2} However, the product from the photoreduction of CO₂ in aqueous solution is usually a mixture that containing CO, H₂, CH₄ and HCOOH,³ because of the multielectron reduction process and the competing H₂ evolution reaction in CO₂ reduction.^{4, 5} Despite continuous efforts have been devoted to exploring efficient photocatalytic CO₂ reduction system, from a practical solar-to-fuels conversion viewpoint, it is desirable to finding catalytic systems that can efficiently transfer CO₂ to a specific product.⁶⁻⁹

Recently, some coordination metal complexes exhibited excellent catalytic performance in photocatalytic selective reduction of CO₂,^{10, 11} owing to their maximum efficiency of catalytic sites and the coordination versatility of the metal centers¹²⁻¹⁵. However, the separation of homogeneous catalysts from the reaction system limited their industrial application. Single site catalysts featuring

atomically distribution of catalytic metal centers on supporters provide a bridge between the homo and heterogeneous catalysis.^{16, 17} In this context, it is imperative to design suitable supporters that not only can accommodate and shield single metal sites but also provide a strong interaction with the metal.¹⁸

The development of covalent organic frameworks (COFs)^{19, 20} opens up new opportunities for catalysis.^{21, 22} Compared to metal-organic-framework (MOF)-based photocatalysts,²³ COF-based photocatalytic materials have unique advantages. The 2D structure of COFs originates from periodic organic building blocks, leading to delocalization of charges in the conjugated framework. The layered nanosheets of 2D COFs not only provide continuous pores for mass transfer, but also offer a fast response to photoexcitation over MOFs with other dimensions continuous. Importantly, the catalytic active sites can be stabilized within the frameworks via the confinement effects and coordination interactions between the confined metal ions/nanoparticles and binding groups in the skeleton of COFs.²⁴⁻²⁶ The well-defined structure and synthetic diversity of COFs enable

control over catalytic active sites in COFs with a precision approaching that of homogeneous metal complex catalysts by modulating the coordination environment of isolated metal centers by changing the coordination group.^{27, 28} In addition, the heteroatom-rich pore walls of COFs not only facilitate CO₂ adsorption,²⁹ but also provide special microenvironments around the coordinated single metal center.³⁰⁻³² Accordingly, using a COF with special coordination microenvironment as a functional supporter for anchoring single metal sites can be expected to bring new opportunities for designing high efficient photocatalyst for selective reduction of CO₂.

In this work, we report a 2,2'-bipyridine-based COF bearing single Ni sites (Ni-TpBpy) as a synergistic catalyst for selective photoreduction of CO₂ to CO (Figure 1). Ni-TpBpy efficiently promoted the selectivity of CO generation in aqueous media, reaching a 4057 μmol g⁻¹ in a 5 h reaction with a 96 % selectivity over H₂ evolution. The good catalytic activity and selectivity of Ni-TpBpy mainly arise from the unique microenvironments around single Ni sites in TpBpy, in which the bipyridine coordination units stabilize the catalytic active Ni center, while the hydrogen-bond interactions between the keto nodes and the Ni-CO₂ reaction intermediate enable the reduction of CO₂ prior to H₂ evolution.

RESULTS AND DISCUSSION

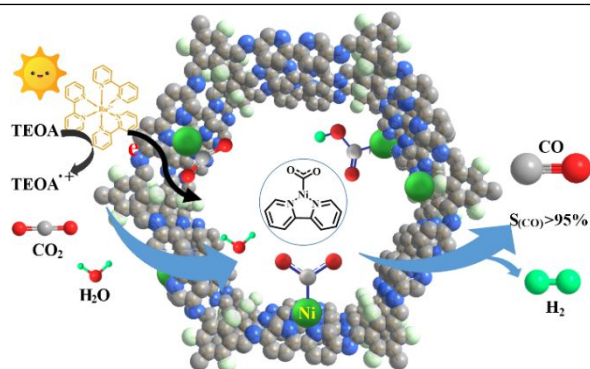


Figure 1. Schematic diagram photocatalytic selective reduction of CO₂ over Ni-TpBpy.

A 2,2'-bipyridine-based COF (TpBpy) was synthesized by the condensation of 1,3,5-triformylphloroglucinol and 5,5'-diamino-2,2'-bipyridine under solvothermal conditions.³³ Ni ions were implanted into TpBpy through a simple treatment of TpBpy with Ni(ClO₄)₂ to yield Ni-TpBpy (Figure 1). FTIR spectroscopy and solid-state ¹³C NMR of Ni-TpBpy are both similar to those observed in TpBpy, revealing the retention of chemical structures during Ni ion loading (Figure S1 and S2). The powder X-ray diffraction (PXRD) shows that the crystalline structure of TpBpy is retained in the Ni-TpBpy (Figure 2a). Further structural details on the coordination of Ni ions into TpBpy are obtained with X-ray photoelectron spectroscopy (XPS) measurements. XPS spectra show the presence of C, N, O and Ni in Ni-TpBpy

(Figure S3). The binding energy of Ni 3p peak at 856 eV is assigned to Ni²⁺ (Figure 2b), indicating the successful loading of Ni ions into the framework. No impurities of other Ni species such as NiO and metallic Ni were evident. In comparison with N 1s XPS spectra of TpBpy, a slight upshift of N 1s peaks in Ni-TpBpy was observed (Figure 2c), which is ascribed to the coordination of nitrogen atoms to Ni ions. The UV-vis diffuse reflectance spectra show that Ni-TpBpy, compared to pristine TpBpy, has a slight red-shift of the absorption edge and a narrow optical band gap probably because of the increased delocalization (Figure S4).³⁰ Scanning electron microscopy (SEM) image shows the original three-dimensional (3D) network morphology of TpBpy is intact after the loading of Ni (Figure S5). Transmission electron microscopy (TEM) images does not exhibit observable nanoparticles of Ni (Figure 2d). The energy-dispersive X-ray (EDX) mapping images of Ni-TpBpy clearly show C, N and Ni are homogeneous distributed in the COF matrix (Figure 2d and S6). The single Ni sites in TpBpy are evidenced by aberration corrected high-angle annular dark-field scanning transmission electron microscopy (HAADF-STEM). As shown in Figure 2e, the bright spots in Ni-TpBpy correspond to the single Ni ions with ultrasmall size (≈0.17 nm), suggesting the atomically dispersed Ni centers in TpBpy.

The porosities of TpBpy and Ni-TpBpy were studied by N₂ adsorption/desorption measurements at 77 K (Figure S7). The Brunauer-Emmett-Teller (BET) surface area and pore volumes were decreased from 973 m² g⁻¹ and 0.6 cm³ g⁻¹ for TpBpy to 580 m² g⁻¹ and 0.4 cm³ g⁻¹ for Ni-TpBpy, respectively. Although the interior cavities of TpBpy are partially filled by Ni ions, the open structure of the TpBpy remained, ensuing reactants accessibility to Ni ions in catalysis. Appreciable amounts of CO₂ adsorption of TpBpy and Ni-TpBpy were also observed (Figure 2f), owing to the combination of microporous character and the heteroatom-rich channels in the framework.²⁹ Interestingly, Ni-TpBpy shows slightly higher CO₂ capture amounts and isosteric heats of adsorption (*Q_{st}*) than those of TpBpy (Inset in Figure 2f), which can be attributed to a Lewis acid-base interaction between the loaded Ni ions and absorbed CO₂ molecules.³⁴

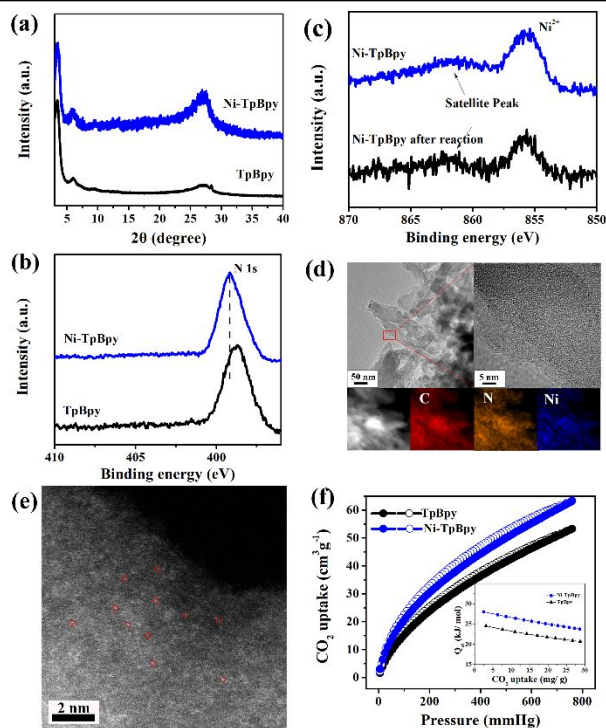


Figure 2. PXRD patterns of TpBpy and Ni-TpBpy (a); Ni 2p XPS spectra of Ni-TpBpy before and after catalytic reaction (b); N 1s XPS spectra of TpBpy and Ni-TpBpy (c); TEM, EDX mapping (d) and aberration-corrected HAADF-STEM (e) images of Ni-TpBpy CO₂ sorption isotherms of the TpBpy and Ni-TpBpy (f). Inset: Isosteric heat of adsorption for CO₂ in TpBpy and Ni-TpBpy.

Considering the catalytic properties of Ni-ligand complexes for CO₂ reduction³⁵ and the high affinity of Ni-TpBpy to CO₂ as well as the excellent chemical stability of TpBpy,³¹ we investigated the photocatalytic CO₂ conversion activity of Ni-TpBpy using [Ru(bpy)₃]Cl₂ (bpy = 2,2'-bipyridine) as a visible-light photosensitizer and triethanolamine (TEOA) as an electron donor in aqueous solution. Figure 3a shows the evolutions of CO and H₂ from Ni-TpBpy catalytic system in a 5-hour photocatalytic reaction. The total amount of CO and H₂ products are 4057 and 170 μmol g⁻¹, respectively, giving a CO selectivity of 96% over completing H₂ generation. The photocatalytic activity is competitive with other previously reported COFs and MOFs, and the catalytic selectivity is among the best based on a review of the recent visible-light-driven heterocatalysts (Table S2).^{6, 30, 36-39} The turnover number of Ni-TpBpy for CO evolution is 13.62 after 5 h irradiation. The apparent quantum efficiency (AQE) for CO evolution at 420 nm is calculated to be 0.3 %. No other CO₂ reduction products (e.g., CH₄, CH₃OH, HCOOH) are detected from the reaction (Figure S8). The participation of CO₂ in the reaction was studied by replacing CO₂ with N₂ under the same reaction conditions. After 4h reaction, no CO was detected (Figure 3b). To confirm the origin of the as-produced CO, isotope experiment was carried out by using ¹³CO₂ as a carbon

source. A peak at m/z = 29 indicates that the produced ¹³CO indeed originated from ¹³CO₂ specie (Figure S9), which evidently confirms that the generated CO comes from CO₂ gas rather than the decomposition of any other organic species in the photocatalytic reaction.

We further conducted the photocatalytic CO₂ reduction reaction under a low CO₂ concentration. A synthetic gas containing 10% CO₂ and 90% Ar was employed to replace pure CO₂. It was found that 915 μmol g⁻¹ of CO with 76% selectivity over H₂ generation can be produced in a 4 h reaction although under a low CO₂ concentration (Inset in Figure 3a).

A series of control experiments were performed to identify the key factors for CO₂-to-CO conversion (Figure 3b). When the CO₂ reduction reaction was conducted in dark, the reaction system is completely inactive to produce any product. The wavelength dependence of CO evolution showed that the trend of CO evolution matches well with the absorption spectrum of the ruthenium complex (Figure S10), further revealing that the CO₂ conversion proceeds by light irradiation. Without Ni-TpBpy or just with TpBpy, negligible CO and H₂ generation were observed, while in the absence of TpBpy, only 4 μmol h⁻¹ CO with 83% selectivity was obtained. In addition, the selectivity of CO over H₂ is influenced by the concentration of H₂O and 2,2'-bipyridine in the reaction solvent (Figure S11 and S12). In comparison, when a physical mixture of Ni ion and TpBpy was used, obviously lower activity and selectivity than those from Ni-TpBpy were observed. TpBpy loaded with other metal ions such as Co²⁺, Fe³⁺, Ru³⁺, Zn²⁺ and Mn²⁺ were also tested in the photocatalytic reduction of CO₂. As shown in Figure 3c, Co ions loaded TpBpy showed a higher photocatalytic activity than that of Ni-TpBpy, however its selectivity only reaches 41% (Inset in Figure 3c), manifesting the feature of integration of single Ni within TpBpy for photocatalytic selective reduction of CO₂ to CO. The production of CO just decreased slightly as the amount of Ni-TpBpy was decreased (Figure S13), suggesting the catalytic efficiency of Ni-TpBpy. Apparently, these results unambiguously demonstrate that single Ni in TpBpy serves as the catalytic sites for conversion CO₂ to CO, and TpBpy boosts the activity and selectivity of photoreduction of CO₂ to CO.

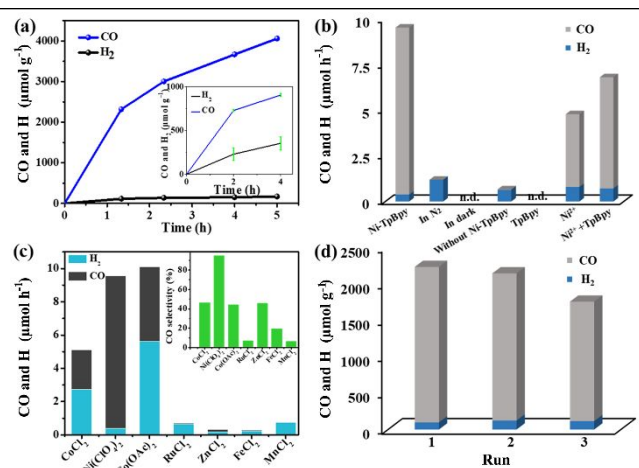


Figure 3. Photocatalytic evolutions of CO and H₂ by Ni-TpBpy under 1 atm and 0.1 atm (diluted with Ar, inset) (a); The research of reaction conditions in a 2 h reaction (b); Different metal ions loaded in TpBpy for CO₂ reduction in a 2 h reaction (c); Stability tests of Ni-TpBpy for selective photoreduction of CO₂ (d).

Cycle experiments revealed that the photocatalytic CO evolution rate could approach up to 966 μmol g⁻¹ h⁻¹ over 3 times in a total of 6 h irradiation time (Figure 3d), which is consistent with the data in the kinetic curves. A slight loss of activity for CO production in the 3rd reaction run may be explained by the coverage of ruthenium species from the degradation of the ruthenium dye on the framework. EDX elemental mappings of the recovered Ni-TpBpy show the appearance of Ru element on the surface of TpBpy (Figure S14). SEM and TEM images show the retention of original 3D network of Ni-TpBpy after cycling reactions. PXRD pattern of the recovered Ni-TpBpy showed a weak long-range order (Figure S15), which can be assigned to the exfoliation of the COF during photocatalysis.⁴⁰ The crystalline structure of the recovered sample can be regenerated by subjecting it to the initial synthesis conditions (Figure S16). No noticeable changes in FTIR (Figure S17), N 1s (Figure S18) and Ni 2p XPS (Figure 2c) spectra between the fresh and recovered Ni-TpBpy demonstrate the chemical stability of Ni-TpBpy. It is noteworthy that after reloading Ni ions onto the recovered TpBpy, the photocatalytic reduction of CO₂ performance can be restored (Figure S19). To test the heterogeneity of Ni-TpBpy, a filtration test was conducted after 2 h of catalysis, after which a significant decrease of activity was observed (Figure S20). The concentration of Ni in the filtered solution was 4.6 ppm as determined by inductively coupled plasma mass spectrometry (ICP), suggesting that only trace of Ni ions existed in reaction system.

To gain mechanistic insight into the photocatalytic reduction of CO₂ by Ni-TpBpy, cyclic voltammetry (CV) was carried out. The growth of the characteristic reduction waves of Ni(bpy)₃²⁺ upon the successive addition of bpy ligand to Ni(ClO₄)₂ solution indicates the

self-assemble formation of Ni(bpy)₃²⁺ (Figure 4a).⁴¹ The CVs of Ni complex in MeCN/H₂O solution show two irreversible reduction waves of Ni complex under both Ar and CO₂ atmosphere (Figure 4b), which can be assigned to the reduction of Ni ions from Ni^{II} to Ni^I and Ni^I to Ni⁰. The catalytic current was emerged under CO₂ atmosphere after the Ni^I to Ni⁰ reduction wave, verifying the reaction of Ni⁰ with CO₂ in the electrochemical process.⁴²

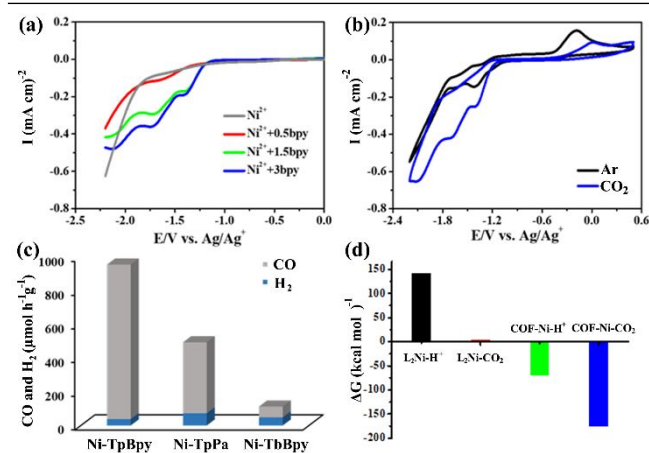


Figure 4. (a) Self-assembly of [Ni(bpy)₃]²⁺ by consecutive addition of bpy to Ni(ClO₄)₂ under a CO₂ atmosphere followed by linear sweep voltammetry (1.0 mM Ni(ClO₄)₂, 0.1 M TBAPF₆ in MeCN/H₂O (3:1) solution, 100 mV s⁻¹); (b) Self-assembled [Ni(bpy)₃]²⁺ under CO₂ or Ar (1.0 mM complex, 0.1 M TBAPF₆ in MeCN/H₂O (3:1) solution, 100 mV s⁻¹, rt); (c) Ni-TpBpy, Ni-TpPa and Ni-TbBpy for Photocatalytic reduction of CO₂ in a 2 h reaction; (d) DFT-calculated relative Gibbs free energy (ΔG, kcal mol⁻¹) with Zero-point correction of CO₂ and H⁺ with and without the optimized building block of TpBpy, L is 2,2'-bipyridine.

To identify the function of the building blocks in TpBpy in improving the selective photoreduction of CO₂ to CO, TpPa without 2,2'-bipyridine units (Figure S21),⁴³ an analogue of TpBpy, was employed into the catalytic reaction. As shown in Figure 4c, Ni loaded TpPa (Ni-TpPa) shows much lower activity and selectivity than Ni-TpBpy, suggesting the importance of bpy units in loading single Ni sites for catalysis. A new COF without keto moieties in the framework, TbBpy, was synthesized by a condensation of 1,3,5-triformylbenzene and 5,5'-diamino-2,2'-bipyridine (Figure S22). Under the identical reaction conditions, only 0.7 μmol CO with a selectivity of 58% was detected by Ni loaded TbBpy (Ni-TbBpy). As the Ni binding sites of TbBpy and TpBpy are similar, the higher catalytic efficiency of TpBpy may be attributed to the keto moieties in TpBpy, which may provide additional effects on the formation of the key intermediate in the catalytic reaction.

Density functional theory (DFT) calculations are further performed to study the catalytic mechanism by Ni-TpBpy. It is known that the adsorption of CO₂ onto the catalyst is the rate-determining step in the photoreduction CO₂ reaction.⁴⁰ The Gibbs free energies of

CO₂ and H₂O on the optimized building block of Ni-TpBpy are calculated. As shown in Figure 4d, the addition of H⁺ to [L₂Ni]⁰ to give L₂Ni-H⁺ adduct cannot easily occur because this reaction is extremely endergonic by 141.4 kcal mol⁻¹ relative to parent [L₂Ni]⁰. The formation of L₂Ni-CO₂ adduct was found at ΔG = 3.2 kcal mol⁻¹, implying the stronger affinity of [L₂Ni]⁰ towards CO₂. Notably, the addition of model compound of the keto unit in TpBpy could significantly decrease the ΔG of the key intermediate, facilitating the formation of Ni-CO₂ adduct, thus leading to an enhanced selectivity of CO product. Noteworthy that the ΔG of CO₂ on Ni-TpBpy is stronger than that of Co-TpBpy, while the ΔG of H₂O on Ni-TpBpy is weaker than that of Ni-TpBpy (Figure S23), suggesting Ni-TpBpy could exhibit superior catalytic activity and selectivity over Co-TpBpy, and Co-TpBpy just could boost the activity of reduction because of the competitive H₂ evolution, which is consistent with the experimental results. The photoreduction process of CO₂ to CO via a carboxyl intermediate on the optimized building block were further calculated. As shown in Figure 5a, a further protonation of Ni-CO₂ adduct to give Ni-COOH adduct is thermodynamically feasible.⁴ The following transformation of Ni-COOH to Ni-CO with H⁺ can proceed facilely, and the release of CO from Ni-CO just need to overcome a rather low barriers. The ΔG for COF-Ni-adducts is much lower than that L₂Ni-adducts, indicating that Ni-TpBpy is kinetically more favorable for the selectivity of CO product.

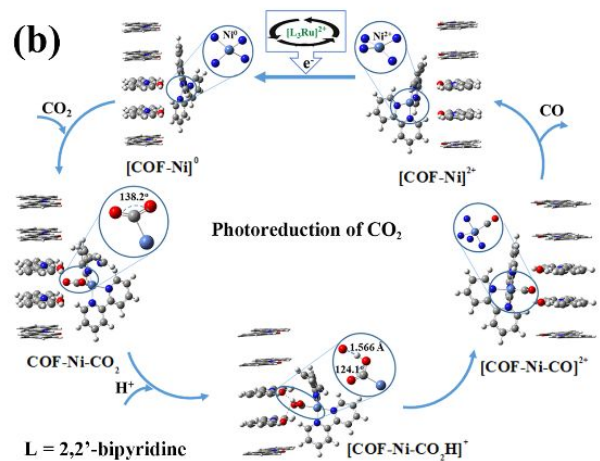
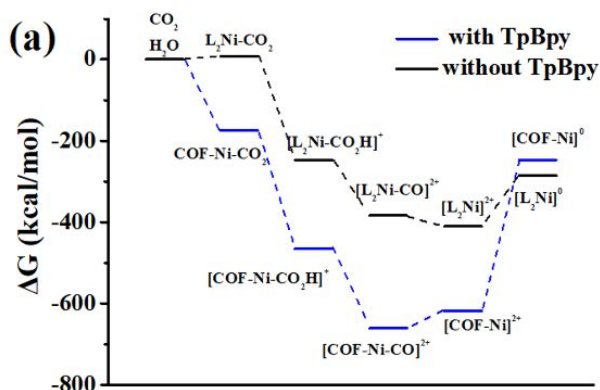


Figure 5. (a) DFT-calculated relative Gibbs free energy (ΔG , kcal mol⁻¹) profiles with Zero-point correction (ZPE) included for the conversion of CO₂ into CO with and without the optimized building block of TpBpy; (b) Proposed reaction mechanism for the photoconversion of CO₂ into CO on Ni-TpBpy.

Based on the experimental and DFT calculations, a possible reaction mechanism for the photocatalytic reduction of CO₂ over Ni-TpBpy is proposed (Figure 5b). Upon visible light irradiation, Ru(bpy)₃²⁺ is excited and transfer electrons to reduce the coordinated CO₂ molecules on Ni-TpBpy. The affinity of CO₂ on Ni sites over H⁺ is crucial for the inhibition of H₂ formation. The coordinated CO₂ in COF-Ni-CO₂ exhibits a bending configuration, confirming that CO₂ was activated by single Ni sites. In intermediate Ni-COOH, one of the C-O bonds elongates to 1.314 Å (Table S1), falling within the typical range of C-O single bond, while the other C-O bond length is 1.221 Å, remaining a double bond. The significantly decreased ΔG of the COF-Ni-CO₂H intermediate is mainly ascribed to the formation of hydrogen bond between COOH and the keto group, thus promoting the stabilization of the key intermediate, and thus enhancing the CO₂ reduction. The results of this calculation explicitly elucidate that single Ni sites in TpBpy truly take the role of the catalytic active sites, where CO₂ molecules are coordinated, activated and reduced, and the TpBpy not only serves as a host for CO₂ molecules and single Ni sites but also contribute to the catalytic activity and selectivity of the reduction of CO₂ to CO, which are in agreement with experimental observations.

CONCLUSION

We demonstrated a design of Ni-TpBpy as a synergistic catalyst for photocatalytic selective conversion of CO₂. Single Ni sites were successfully anchored in TpBpy through the chelation of bipyridine binding units. Ni-TpBpy exhibits excellent photocatalytic selective reduction of CO₂ to CO either in pure or diluted CO₂, which are mainly ascribed to the synergistic effects of single Ni catalytic site and TpBpy supporter. Control experiments and theoretical calculations indicated that both bipyridine coordination units and the keto nodes in TpBpy play key roles in stabilization of single Ni sites, activation and conversion of CO₂ in the catalytic reaction. This work strongly highlights the considerable potential of COFs for fabrication of single-site catalysts, and should be simulate the development of novel photocatalysts through delicate design of their coordination microenvironments around the catalytic active sites.

EXPERIMENTAL SECTION

Synthesis of TpBpy. TpBpy was prepared according to literature methods with a little modification.³³ A Pyrex tube was charged with triformylphloroglucinol (21 mg,

0.10 mmol) and 5,5'-diamino-2,2'-bipyridine (27.9 mg, 0.15 mmol) in 1.1 mL of a 5:5:1 v:v solution of 1,4-dioxane: mesitylene: 6 M aqueous acetic acid. This mixture was sonicated for 10 minutes in order to get a homogenous dispersion. The tube was flash frozen at 77 K (liquid N₂ bath), evacuated and flame-sealed. The reaction mixture was heated at 120 °C for 5 days to afford an orange-red precipitate. The precipitate was isolated by filtration and dried under vacuum at 60 °C overnight to afford TpBpy (40 mg, 82%).

Synthesis of Ni-TpBpy. TpBpy (50 mg) was treated with Ni(ClO₄)₂·6H₂O (30 mg) in 20 ml acetonitrile. The solution was stirred for 8h at room temperature. The solid was filtered washed with copious amount of acetonitrile and dried in vacuum at 60 °C overnight to give Ni-TpBpy. Ni content in Ni-TpBpy was 0.3 mmol g⁻¹ as determined by ICP.

Synthesis of TpPa. TpPa was prepared according to literature methods with a little modification.³⁹ A Pyrex tube was charged with triformylphloroglucinol (63 mg, 0.3 mmol), paraphenylenediamine (48 mg, 0.45 mmol) in 3.5 mL of a 3:3:1 v:v solution of 1,4-dioxane: mesitylene: 3 M aqueous acetic acid. This mixture was sonicated for 10 minutes in order to get a homogenous dispersion. The tube was then flash frozen at 77 K (liquid N₂ bath) and degassed by three freeze-pump-thaw cycles. The tube was sealed off and then heated at 120 °C for 3 days. The red precipitate was collected by filtration and washed with anhydrous acetone. The powder collected and then dried at 120 °C under vacuum to afford TpPa (89 mg, 80%).

Synthesis of TbBpy. A Pyrex tube was charged with 1,3,5-triformylbenzene (16 mg, 0.10 mmol) and 5,5'-diamino-2,2'-bipyridine (27.9 mg, 0.15 mmol) in 1.1 mL of a 9:1:1 v:v solution of 1,4-dioxane: mesitylene: 6 M aqueous acetic acid. The tube was flash frozen at 77 K (liquid N₂ bath), evacuated and flame-sealed. The reaction mixture was heated at 120 °C for 3 days to afford a yellow precipitate. The precipitate was isolated by filtration and dried under vacuum at 80 °C overnight to afford TbBpy (30 mg, 70%).

Photocatalytic reduction of CO₂. A mixed solution of acetonitrile, H₂O and TEOA (3:1:1, 5 mL) containing Ni-TpBpy (10 mg) 2,2'-bipyridine (15 mg, 0.1 mmol) and [Ru(bpy)₃]Cl₂·6H₂O (6.5 mg, 0.01 mmol) were purged with CO₂ for 15 min. The solution was then irradiated under a xenon lamp (300 W) with a UV-cutoff filter (λ ≥ 420 nm) at 298 K. After each reaction time, the generated gas in the headspace of the reaction vessel was sampled with a gas-tight syringe and determined by gas chromatography (Agilent 7890B) with both TCD and FID detectors. H₂ was detected using a TCD. CO was converted to CH₄ by a methanation reactor and then analyzed by FID. The apparent quantum efficiency (AQE) at 420 nm was calculated by the following equation: AQE = (2×amount of CO molecules evolved in 2h/number of incident photons in 2h)×100%.

Stability tests of Ni-TpBpy for photoreduction of CO₂. Three runs of consecutive photocatalytic reduction

of CO₂ to CO by adding equal amounts of [Ru(bpy)₃]Cl₂·6H₂O at each run (0.01 mmol of [Ru(bpy)₃]Cl₂·6H₂O were carried out in 30 μL CH₃CN and 10 μL H₂O) to the photocatalytic system after 2 h of reaction and re-introducing CO₂, and then the mixture was irradiated under a xenon lamp (300 W) with a UV-cutoff filter (λ ≥ 420 nm) at 298 K.

Electrochemical measurements. Cyclic voltammetry on Ni(ClO₄)₂·6H₂O and 2,2'-bipyridine was carried out in a mixed solution of MeCN/H₂O (3:1 v/v) containing 0.10 M tetrabutylammonium hexafluorophosphate (TBAPF₆) as an electrolyte at 298 K under Ar or CO₂ with use of a glassy carbon as a working electrode, a platinum wire as a counter electrode, and a Ag/AgCl electrode.

ASSOCIATED CONTENT

Supporting Information. Materials, methods, detailed characterization of TpBpy, Ni-TpBpy, TpPa and TbBpy, DFT calculations. This material is available free of charge via the Internet at <http://pubs.acs.org>.

AUTHOR INFORMATION

Corresponding Author

* lyli@fzu.edu.cn
* yuyan@fzu.edu.cn
* zgzou@nju.edu.cn

Author Contributions

W. Zhong and R. Sa contributed equally.

Notes

The authors declare no competing financial interest.

ACKNOWLEDGMENT

We thank the National Natural Science Foundation of China (No. 51672046, 51672047 and 21403238), Natural Science Foundation of Fujian Province of China (No. 2019J01226, 2019J01648), Open Project Program of the State Key Laboratory of Photocatalysis on Energy and Environment (No. SKLPEE-KF201815, SKLPEE-KF201813).

REFERENCES

- (1) White, J. L.; Baruch, M. F.; Pander, J. E.; Hu, Y.; Fortmeyer, I. C.; Park, J. E.; Zhang, T.; Liao, K.; Gu, J.; Yan, Y.; Shaw, T. W.; Abelev, E.; Bocarsly, A. B. Light-driven heterogeneous reduction of carbon dioxide: Photocatalysts and photoelectrodes. *Chem. Rev.* **2015**, *115*, 12888.
- (2) Inoue, T.; Fujishima, A.; Konishi, S.; Honda, K. Photoelectrocatalytic reduction of carbon dioxide in aqueous suspensions of semiconductor powders. *Nature* **1979**, *277*, 637.
- (3) Li, X.; Yu, J.; Jaroniec, M.; Chen, X. Cocatalysts for selective photoreduction of CO₂ into solar fuels. *Chem. Rev.* **2019**, *119*, 3962.
- (4) Men, Y. L.; You, Y.; Pan, Y. X.; Gao, H.; Xia, Y.; Cheng, D. G.; Song, J.; Cui, D. X.; Wu, N.; Li, Y.; Xin, S.; Goodenough, J. B. Selective co evolution from photoreduction of CO₂ on a metal-carbide-based composite catalyst. *J. Am. Chem. Soc.* **2018**, *140*, 13071.
- (5) Fu, Y.; Sun, D.; Chen, Y.; Huang, R.; Ding, Z.; Fu, X.; Li, Z. An amine-functionalized titanium metal-organic framework

photocatalyst with visible-light-induced activity for CO₂ reduction. *Angew. Chem., Int. Ed.* **2012**, *51*, 3364.

(6) Niu, K. Y.; Xu, Y.; Wang, H. C.; Ye, R.; Xin, H. L.; Lin, F.; Tian, C. X.; Lum, Y. W.; Bustillo, K. C.; Doeff, M. M.; Koper, M. T. M.; Ager, J.; Xu, R.; Zheng, H. M. A spongy nickel-organic CO₂ reduction photocatalyst for nearly 100% selective CO production. *Sci. Adv.* **2017**, *3*, 1700921.

(7) Wang, Y.; Zhang, Z.; Zhang, L.; Luo, Z.; Shen, J.; Lin, H.; Long, J.; Wu, J. C. S.; Fu, X.; Wang, X.; Li, C. Visible-light driven overall conversion of CO₂ and H₂O to CH₄ and O₂ on 3D-SiC@2D-MoS₂ heterostructure. *J. Am. Chem. Soc.* **2018**, *140*, 14595.

(8) Wu, X.; Li, Y.; Zhang, G.; Chen, H.; Li, J.; Wang, K.; Pan, Y.; Zhao, Y.; Sun, Y.; Xie, Y. Photocatalytic CO₂ conversion of M_{0.33}WO₃ directly from the air with high selectivity: Insight into full spectrum-induced reaction mechanism. *J. Am. Chem. Soc.* **2019**, *141*, 5267.

(9) Han, Q.; Bai, X.; Man, Z.; He, H.; Li, L.; Hu, J.; Alsaedi, A.; Hayat, T.; Yu, Z.; Zhang, W.; Wang, J.; Zhou, Y.; Zou, Z. Convincing synthesis of atomically thin, single-crystalline InVO₄ sheets toward promoting highly selective and efficient solar conversion of CO₂ into CO. *J. Am. Chem. Soc.* **2019**, *141*, 4209.

(10) Kuramochi, Y.; Ishitani, O.; Ishida, H. Reaction mechanisms of catalytic photochemical CO₂ reduction using Re(I) and Ru(II) complexes. *Coord. Chem. Rev.* **2017**, *373*, 333.

(11) Bonin, J.; Maurin, A.; Robert, M. Molecular catalysis of the electrochemical and photochemical reduction of CO₂ with Fe and Co metal based complexes. Recent advances. *Coord. Chem. Rev.* **2017**, *334*, 184.

(12) Rao, H.; Schmidt, L. C.; Bonin, J.; Robert, M. Visible-light-driven methane formation from CO₂ with a molecular iron catalyst. *Nature* **2017**, *548*, 74.

(13) Ouyang, T.; Huang, H. H.; Wang, J. W.; Zhong, D. C.; Lu, T. B. A dinuclear cobalt cryptate as a homogeneous photocatalyst for highly selective and efficient visible-light driven CO₂ reduction to CO in CH₃CN/H₂O solution. *Angew. Chem., Int. Ed.* **2017**, *56*, 738.

(14) Takeda, H.; Kamiyama, H.; Okamoto, K.; Irimajiri, M.; Mizutani, T.; Koike, K.; Sekine, A.; Ishitani, O. Highly efficient and robust photocatalytic systems for CO₂ reduction consisting of a Cu(I) photosensitizer and Mn(I) catalysts. *J. Am. Chem. Soc.* **2018**, *140*, 17241.

(15) Cui, X.; Wang, J.; Liu, B.; Ling, S.; Long, R.; Xiong, Y. Turning Au nanoclusters catalytically active for visible-light-driven CO₂ reduction through bridging ligands. *J. Am. Chem. Soc.* **2018**, *140*, 16514.

(16) Qiao, B.; Wang, A.; Yang, X.; Allard, L. F.; Jiang, Z.; Cui, Y.; Liu, J.; Li, J.; Zhang, T. Single-atom catalysis of CO oxidation using Pt₁/FeOx. *Nat. Chem.* **2011**, *3*, 634.

(17) Chen, F.; Jiang, X.; Zhang, L.; Lang, R.; Qiao, B. Single-atom catalysis: Bridging the homo- and heterogeneous catalysis. *Chin. J. Catal.* **2018**, *39*, 893.

(18) Huang, P.; Huang, J.; Pantovich, S. A.; Carl, A. D.; Fenton, T. G.; Caputo, C. A.; Grimm, R. L.; Frenkel, A. I.; Li, G. Selective CO₂ reduction catalyzed by single cobalt sites on carbon nitride under visible-light irradiation. *J. Am. Chem. Soc.* **2018**, *140*, 16042.

(19) Huang, N.; Wang, P.; Jiang, D. Covalent organic frameworks: A materials platform for structural and functional designs. *Nat. Rev. Mater.* **2016**, *1*, 16068.

(20) Cote, A. P.; Benin, A. I.; Ockwig, N. W.; O'Keeffe, M.; Matzger, A. J.; Yaghi, O. M. Porous, crystalline, covalent organic frameworks. *Science* **2005**, *310*, 1166.

(21) Rogge, S. M. J.; Bavykina, A.; Hajek, J.; Garcia, H.; Olivos-Suarez, A. I.; Sepulveda-Escribano, A.; Vimont, A.; Clet, G.; Bazin, P.; Kapteijn, F.; Daturi, M.; Ramos-Fernandez, E. V.; Llabres, I. X. F. X.; Van Speybroeck, V.; Gascon, J. Metal-organic

and covalent organic frameworks as single-site catalysts. *Chem. Soc. Rev.* **2017**, *46*, 3134.

(22) Lin, C. Y.; Zhang, D.; Zhao, Z.; Xia, Z. Covalent organic framework electrocatalysts for clean energy conversion. *Adv. Mater.* **2018**, *30*, 1703646.

(23) Li, R.; Zhang, W.; Zhou, K. Metal-organic-framework-based catalysts for photoreduction of CO₂. *Adv. Mater.* **2018**, *30*, 1705512.

(24) Ding, S. Y.; Gao, J.; Wang, Q.; Zhang, Y.; Song, W. G.; Su, C. Y.; Wang, W. Construction of covalent organic framework for catalysis: Pd/COF-LZU1 in Suzuki-Miyaura coupling reaction. *J. Am. Chem. Soc.* **2011**, *133*, 19816.

(25) Lu, S.; Hu, Y.; Wan, S.; McCaffrey, R.; Jin, Y.; Gu, H.; Zhang, W. Synthesis of ultrafine and highly dispersed metal nanoparticles confined in a thioether-containing covalent organic framework and their catalytic applications. *J. Am. Chem. Soc.* **2017**, *139*, 17082.

(26) Cui, K.; Zhong, W.; Li, L.; Zhuang, Z.; Li, L.; Bi, J.; Yu, Y. Well-defined metal nanoparticles@covalent organic framework yolk-shell nanocages by ZIF-8 template as catalytic nanoreactors. *Small* **2019**, *15*, 1804419.

(27) Rozhko, E.; Bavykina, A.; Osadchii, D.; Makkee, M.; Gascon, J. Covalent organic frameworks as supports for a molecular Ni based ethylene oligomerization catalyst for the synthesis of long chain olefins. *J. Catal.* **2017**, *345*, 270.

(28) Banerjee, T.; Haase, F.; Savasci, G.; Gottschling, K.; Ochsenfeld, C.; Lotsch, B. V. Single-site photocatalytic H₂ evolution from covalent organic frameworks with molecular cobaloxime co-catalysts. *J. Am. Chem. Soc.* **2017**, *139*, 16228.

(29) Zeng, Y.; Zou, R.; Zhao, Y. Covalent organic frameworks for CO₂ capture. *Adv. Mater.* **2016**, *28*, 2855.

(30) Yang, S.; Hu, W.; Zhang, X.; He, P.; Pattengale, B.; Liu, C.; Cendejas, M.; Hermans, I.; Zhang, X.; Zhang, J.; Huang, J. 2D covalent organic frameworks as intrinsic photocatalysts for visible light-driven CO₂ reduction. *J. Am. Chem. Soc.* **2018**, *140*, 14614.

(31) Aiyappa, H. B.; Thote, J.; Shinde, D. B.; Banerjee, R.; Kurungot, S. Cobalt-modified covalent organic framework as a robust water oxidation electrocatalyst. *Chem. Mater.* **2016**, *28*, 4375.

(32) Fu, Y.; Zhu, X.; Huang, L.; Zhang, X.; Zhang, F.; Zhu, W. Azine-based covalent organic frameworks as metal-free visible light photocatalysts for CO₂ reduction with H₂O. *Appl. Catal. B: Environ* **2018**, *239*, 46.

(33) Shinde, D. B.; Aiyappa, H. B.; Bhadra, M.; Biswal, B. P.; Wadge, P.; Kandambeth, S.; Garai, B.; Kundu, T.; Kurungot, S.; Banerjee, R. A mechanochemically synthesized covalent organic framework as a proton-conducting solid electrolyte. *J. Mater. Chem.* **2016**, *4*, 2682.

(34) Dietzel, P. D.; Johnsen, R. E.; Fjellvag, H.; Bordiga, S.; Groppo, E.; Chavan, S.; Blom, R. Adsorption properties and structure of CO₂ adsorbed on open coordination sites of metal-organic framework Ni₂(DHTP) from gas adsorption, IR spectroscopy and X-ray diffraction. *Chem Commun* **2008**, 5125.

(35) Wang, J. W.; Liu, W. J.; Zhong, D. C.; Lu, T. B. Nickel complexes as molecular catalysts for water splitting and CO₂ reduction. *Coord. Chem. Rev.* **2019**, *378*, 237.

(36) Wang, S.; Yao, W.; Lin, J.; Ding, Z.; Wang, X. Cobalt imidazolate metal-organic frameworks photosplit CO₂ under mild reaction conditions. *Angew. Chem., Int. Ed.* **2014**, *53*, 1034.

(37) Choi, K. M.; Kim, D.; Rungtaweeworanit, B.; Trickett, C. A.; Barmanbek, J. T.; Alshammari, A. S.; Yang, P.; Yaghi, O. M. Plasmon-enhanced photocatalytic CO₂ conversion within metal-organic frameworks under Visible Light. *J. Am. Chem. Soc.* **2017**, *139*, 356.

1 (38) Zhu, W.; Zhang, C.; Li, Q.; Xiong, L.; Chen, R.; Wan, X.;
2 Wang.; Chen, Z. W.; Deng, Z.; Peng, Y. Selective reduction of
3 CO₂ by conductive MOF nanosheets as an efficient co-catalyst
4 under visible light illumination. *Appl. Catal. B: Environ.* **2018**,
5 238, 339.

6 (39) Han, B.; Ou, X.; Deng, Z.; Song, Y.; Tian, C.; Deng, H.; Xu,
7 Y. J.; Lin, Z. Nickel metal-organic framework monolayers for
8 photoreduction of diluted CO₂: Metal-node-dependent activity
9 and selectivity. *Angew. Chem., Int. Ed.* **2018**, 57, 16811.

10 (40) Stegbauer, L.; Schwinghammer, K.; Lotsch, B. V. A
11 hydrazone-based covalent organic framework for photocatalytic
12 hydrogen production. *Chem. Sci.* **2014**, 5, 2789.

13 (41) Kuehnel, M. F.; Orchard, K. L.; Dalle, K. E.; Reisner, E.
14 Selective photocatalytic CO₂ reduction in water through
15 anchoring of a molecular Ni catalyst on CdS nanocrystals. *J. Am.*
16 *Chem. Soc.* **2017**, 139, 7217.

(42) Hong, D.; Tsukakoshi, Y.; Kotani, H.; Ishizuka, T.;
Kojima, T. Visible-light-driven photocatalytic CO₂ reduction by a
Ni(II) complex bearing a bioinspired tetradentate ligand for
selective CO production. *J. Am. Chem. Soc.* **2017**, 139, 6538.

(43) Kandambeth, S.; Mallick, A.; Lukose, B.; Mane, M. V.;
Heine, T.; Banerjee, R. Construction of crystalline 2D covalent
organic frameworks with remarkable chemical (acid/base)
stability via a combined reversible and irreversible route. *J. Am.*
Chem. Soc. **2012**, 134, 19524.

TOC

